

Mapping Antarctic ozone from visible-channel data

Robert D. Boime and Stephen G. Warren

Department of Atmospheric Sciences AK-40
University of Washington, Seattle, Washington 98195, USA

ABSTRACT

Accurate, detailed maps of total ozone were not available until the launch of the Total Ozone Mapping Spectrometer (TOMS) in late 1978. However, the Scanning Radiometer (SR) on NOAA satellites during the 1970s included a visible channel that overlapped closely with the Chappuis absorption band of ozone around 600 nm. The Antarctic atmosphere and surface contain no other significant absorbers of radiation at those wavelengths, which makes Antarctica an ideal region to isolate the ozone signal in the visible-channel data. We are investigating whether SR data can be used to map Antarctic ozone prior to 1978.

We use a simple calculation of two-way transmittance to obtain total ozone from data taken by the Advanced Very High Resolution Radiometer (AVHRR). The AVHRR was the successor to the SR on NOAA satellites, and because it flew during the 1980s, we are able to compare our derived ozone amounts with those derived from TOMS. Our method works only over scenes whose albedos are large and unvarying.

Sections 1-3 of this report are similar to our report¹ in the *Proceedings of the Quadrennial Ozone Symposium*; Section 4 describes progress made during the past year. Significant improvement resulted from rejecting samples with extremely high or low reflectance (probably cloud edges), so that we solve for ozone amount only over a background of snow or uniform cloud. The root-mean-square (rms) error in AVHRR-derived total ozone (relative to TOMS) was 34-50 Dobson Units (DU). Further improvement resulted from incorporating a preliminary bidirectional reflectance function, reducing the rms error to 28-35 DU.

We are now modifying our retrieval method to include a comprehensive bidirectional reflectance function for the surface and for uniform clouds, and to choose the appropriate scales for spatial and temporal averaging. If the method appears useful after these improvements have been made, the technique can be applied to SR data from the 1970s.

1. INTRODUCTION

The Antarctic ozone hole appears to have developed rapidly beginning about the same time that the Total Ozone Mapping Spectrometer (TOMS) was launched in late 1978. Evidence for ozone changes prior to that time is limited to ground-based measurements from a few Antarctic stations and unreliable satellite data, which suggest a slow decrease during the 1970s. The ozone amounts mapped by TOMS show large spatial and temporal variation on scales of a few hundred kilometers and a few days.² A few isolated stations therefore cannot adequately represent the entire continent, so it would be useful to find a method to map the spatial variation of total ozone over Antarctica prior to 1978.

Radiometer data from NOAA polar-orbiting satellites may contain information about the early evolution of the ozone hole above Antarctica. These instruments have a visible channel that overlaps with a weak absorption band of ozone at 600-nm wavelength (Figure 1), where the other constituents in the Antarctic atmosphere and surface, including clouds and snow, are non-absorptive. The visible-channel data have been gridded and

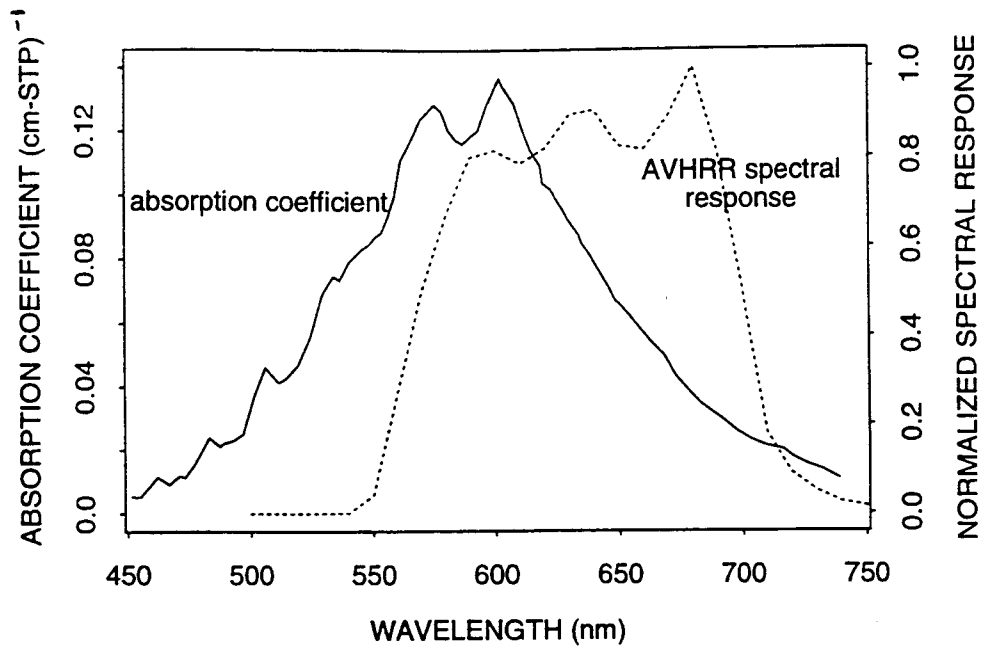


Figure 1. The Chappuis absorption band of ozone and the spectral response of the AVHRR visible channel on the NOAA-9 spacecraft. The absorption coefficients for the Chappuis band are taken from Vigroux,⁸ and the channel response values from Rossow *et al.*³

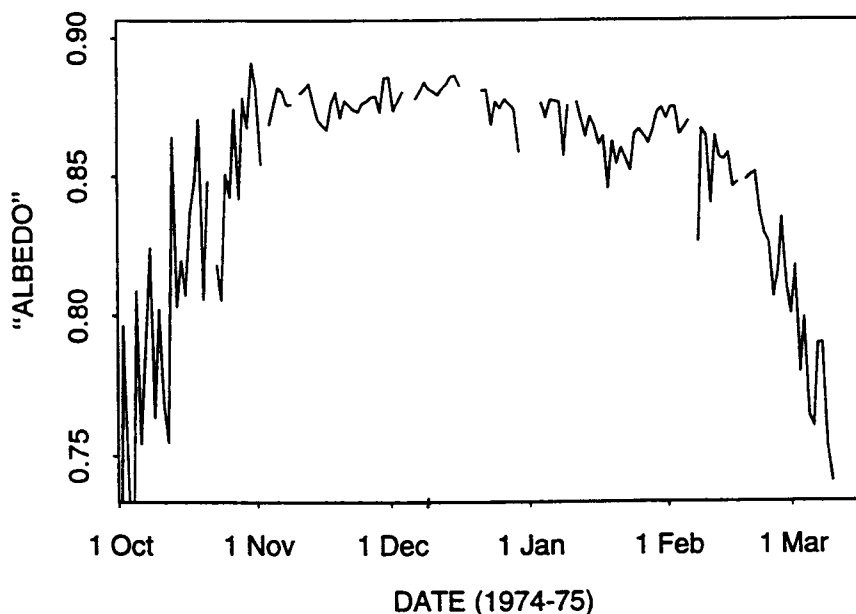


Figure 2. Daily values of "albedo" (assuming isotropic reflectance) from September 1974 to March 1975 at South Pole. The albedo rises from 0.78 in October to 0.88 in December, about what one would expect for a normal unchanging column ozone amount of 300 DU (Figure 2 of Reference 9). The lower albedo in October is due to the longer slant path through the ozone at low solar elevation angles. The data were taken by Channel 1 of the Scanning Radiometer (SR), the predecessor to the Advanced Very High Resolution Radiometer (AVHRR). [Figure obtained from A. Gruber, NOAA-NESDIS.]

archived by NOAA beginning 1974, and the early measurements do show decreasing absorption as solar elevation increases (Figure 2). This dependence is apparently due to the shorter slant path through the ozone layer with increasing solar elevation, indicating that visible absorption by ozone is indeed significant so that variations in ozone amount should be detectable.

To evaluate the method's feasibility, we analyze satellite data taken during October-December 1987 by the AVHRR on NOAA-9. The calculation incorporates only absorption by ozone and reflection by the clouds and snow below. Use of the 1980s data allows a comparison between our retrieved ozone amounts with those from TOMS. [Because there is only one visible channel on the NOAA satellites, we cannot make use of a differential absorption method such as those employed in the UV by TOMS and by the Dobson spectrophotometers to measure total ozone.]

The AVHRR has a spatial resolution of 1.1 km and an intensity count resolution of 0.1% (ten bits). However, in order to obtain large spatial and temporal coverage, it is convenient in this initial test to use the "level B3" data of the International Satellite Cloud Climatology Project³ (ISCCP). For the B3 archive, the original 1.1-km data are sampled to 30-km resolution, and the 10-bit counts are truncated to 8 bits.

2. METHOD

The simplest possible method for deriving total ozone amount from a visible-channel measurement uses a calculation of two-way transmittance:

$$I = (Q_0 A_s \chi / \pi) \cos \theta_o \exp\{-0.0827u [x(\theta_o) + \sec \theta]\} \quad (1)$$

Q_0 is a fraction of the solar constant: the integral of the incident solar spectral irradiance at the top of the atmosphere normal to the solar beam, weighted by the channel sensitivity function (Figure 1). Radiation from the sun passes through the ozone layer of vertical thickness u (cm-STP), along pathlength x , a function of solar zenith angle θ_o . Large solar zenith angles are typical in Antarctic latitudes, so the effect of Earth's curvature must be taken into account when calculating pathlength. The function $x(\theta_o)$ is given by Rozenberg⁴:

$$x = [\cos \theta_o + 0.025 \exp(-11 \cos \theta_o)]^{-1} \quad (2)$$

Note that when $\theta_o < 70^\circ$, $x \approx \sec \theta_o$.

After the solar beam has passed through the ozone layer, it encounters everything beneath the layer, including clouds and snow. The sub-ozone layer has albedo A_s and anisotropic reflectance factor χ : a function of θ_o , θ , and ϕ , where θ is the satellite zenith angle and ϕ is the relative azimuth angle between sun and satellite. χ is proportional to the bidirectional reflectance distribution function, and is defined such that its average value over the upward hemisphere is 1.0. The reflected radiation passes through the ozone layer again at angle θ to reach the satellite. Given a measurement of intensity I by the radiometer, equation (1) is solved for u . The units are $W \text{ m}^{-2} \text{ sr}^{-1}$ for intensity I , $W \text{ m}^{-2}$ for irradiance Q_0 , and sr for π .

The ozone absorption coefficient in (1) is $0.0827 \text{ (cm-STP)}^{-1}$, which is an average of the Chappuis band (Figure 1), weighted by the NOAA-9 AVHRR visible channel-function (also shown in Figure 1) and the solar spectral irradiance. [This coefficient differs slightly from the value used previously¹ because the solar-spectrum weighting was neglected there.] This absorption coefficient will differ somewhat for different satellites, because of differences in their channel-functions.

Over dark surfaces, variations in u or θ_0 have little effect on the planetary albedo at 600-nm wavelength because most of the radiation not absorbed by ozone is absorbed by the underlying surface. Uniform snow surfaces, however, have very high albedo at 600 nm, about 0.97 (Ref. 5), which is the value we use for A_s . The near-infrared albedo is much lower, giving the familiar value for spectrally-averaged solar albedo of 80-85% for Antarctic snow. Because the visible surface albedo is already so high, clouds do not significantly increase the top-of-atmosphere albedo.

Equation (1) neglects scattering by the atmosphere above the ozone layer. Polar stratospheric clouds can exist within and partially above the ozone layer, but their typical optical depth⁶ is only about 0.01. The optical depth is somewhat greater over mountainous areas, but our method has other difficulties in those regions as well. Rayleigh scattering is weak at 600 nm, and only a few percent of the atmospheric mass is above the ozone, so it is ignored as well. The effect of Rayleigh scattering *below* the ozone layer will most likely cause the anisotropic reflectance factor χ for the sub-ozone scene to be slightly more isotropic than that of the snow or cloud surface. Rayleigh scattering is implicitly included in our method when we obtain χ from satellite observations, but its effect will have to be incorporated explicitly when we (in the future) use a χ from surface observations, as discussed below.

Due to the limited spatial and intensity resolution in the ISCCP-B3 data used for this initial test, the uncertainty in θ_0 , θ , and I result in an inherent uncertainty of 60 Dobson units (DU) for each derived u value. However, the satellite passes above the polar regions several times per day, and the pixel size is on the order of tens of kilometers while ozone varies over a few hundred kilometers. Approximately 100 derived u values can therefore be binned and averaged into a single value on any given day without loss of map resolution. Random error due to finite data resolution is then reduced to 6 DU per mapped u value. This is smaller than the error due to inadequate knowledge of χ .

3. REFLECTION FROM CLOUDS AND SNOW

At most Antarctic locations, the most uncertain quantity in (1) is the anisotropic reflectance factor χ of the sub-ozone layer. The retrieved ozone amount is sensitive to χ because the visible absorption by ozone is so weak. Typically, the derived total column ozone increases by 50-100 DU with a few-percent increase in the assumed value of χ in the satellite's direction. [The direction of the satellite with respect to the pixel being scanned is defined by θ and ϕ .]

Small longitudinal dunes called sastrugi cover nearly the entire Antarctic ice sheet. They cause χ to depend not only θ_0 , θ , and ϕ , but also on the azimuth of the sun relative to the prevailing wind direction. Because the dunes align themselves parallel to the wind, the

sastrugi axis is close to the prevailing wind direction. A flat snow surface has a forward-peaked χ like most natural surfaces. This normal forward-scattering pattern also results from a sastrugi field when the solar beam is parallel to the sastrugi axis, but a reduction in the strength of the forward peak results when the solar beam is perpendicular to the sastrugi axis. The sastrugi vary in orientation and height across Antarctica. Their predominant orientations are fairly well established and have been mapped by Parish and Bromwich⁷. In our development of the ozone-remote-sensing method to date, we are not taking sastrugi into account.

Although clouds do not change the top-of-atmosphere albedo by much over a snow surface (at visible wavelengths), they may change χ significantly. Cloud edges often appear much brighter or darker than the interior cloud field, so we develop a procedure below to reject cloud-edge samples. However, even uniform clouds may alter χ to some extent. Clouds tend to scatter radiation in the forward direction. Putting a uniform cloud over a flat snow surface would change χ very little since flat snow tends to be forward-scattering also. But as discussed above, sastrugi can alter the scattering pattern. In regions with large sastrugi (near the margins of the ice sheet where the surface slopes down toward the ocean), it will therefore probably be important in future work to find a way either to detect clouds or to remove their influence. This may possibly be done by making use of the fact that cloud cover has a higher frequency of variability in time than does total ozone.

4. AVHRR-DERIVED OZONE AMOUNTS, COMPARED TO TOMS

Figures 3-5 show time series of total ozone derived from AVHRR and TOMS in three 100x100 km grid-boxes over East Antarctica, to illustrate the stepwise improvements we have made in the analysis procedure. [The TOMS plots (dashed lines) in Figures 4 and 5 are the same as in Figure 3.] Figure 3 (a,b) is essentially identical to Figure 3 of Reference 1. That analysis used a constant value of $\chi=0.9$ independent of sun angle, satellite angle, or season, chosen from limited surface measurements of bidirectional reflectance as being typical for the range of values of θ_0 , θ , and ϕ encountered in the data for 1987. Figure 3c here differs from Figure 3c of Reference 1 in using a more appropriate value $\chi=1.0$ at the South Pole, and also because the grid box is smaller.

The errors apparent in Figure 3 are of two types: (1) the day-to-day variability in the AVHRR-derived ozone amounts is too large, and (2) the seasonal trend is too large. The first type of error is largely due to the influence of some anomalously bright or dark samples entering the grid-box averages. Examination of AVHRR images of Antarctica suggests that these extreme brightness values occur at cloud edges, the sun-facing edge being brighter than average (because of more-normal solar incidence) and the far edge darker (because part of the scene viewed is the cloud's shadow on the snow surface).

We therefore introduced a cloud-edge-rejection criterion into the analysis procedure. All the raw brightness values were converted to reflectances, and both tails of the reflectance distribution were rejected. The rejection criterion was chosen as that which minimized the rms-error in derived ozone amounts for the entire seasonal time-series at these three locations. We also rejected data for solar elevations below 30°; they are noisy due both to low light levels and to extreme (and poorly known) values of χ at large θ_0 . Figure 4 shows that these procedures reduced the noise considerably, but required rejection of 25-44% of the individual raw data samples.

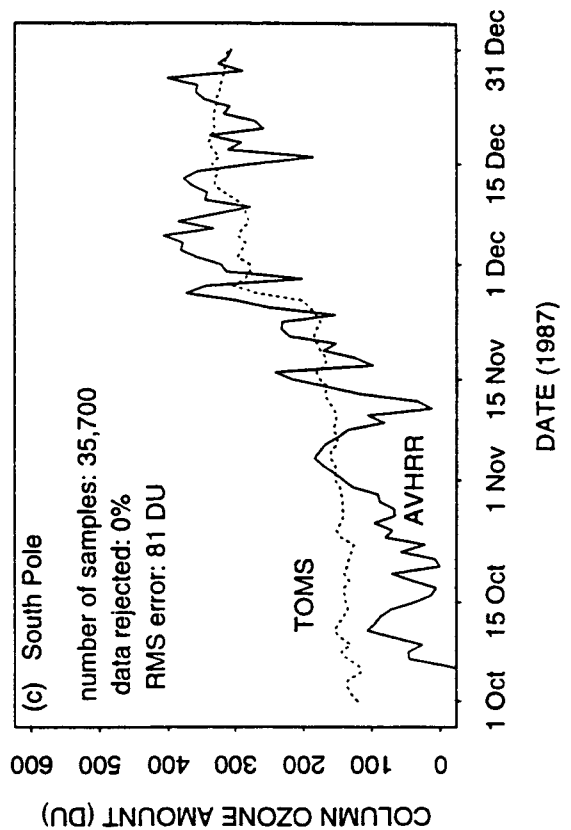
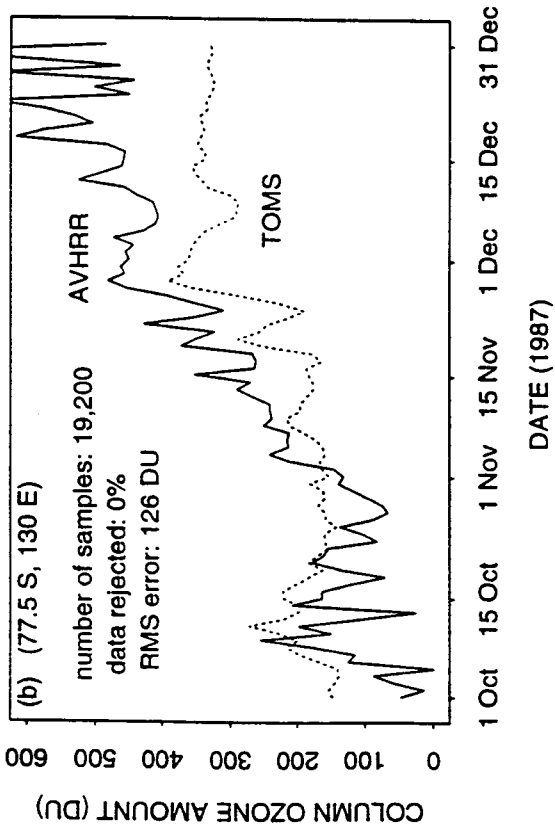
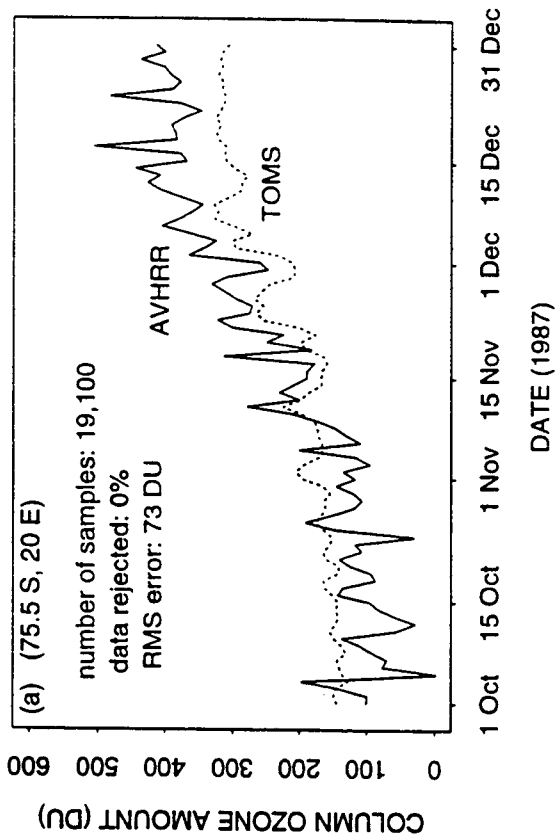


Figure 3. FIRST ALGORITHM. Time series from 1 October to 31 December 1987 of total ozone derived from the visible channel of AVHRR and from TOMS at three locations, using a constant value for χ and no rejection of cloud edges. This figure is essentially the same as Figure 3 of Reference 1.

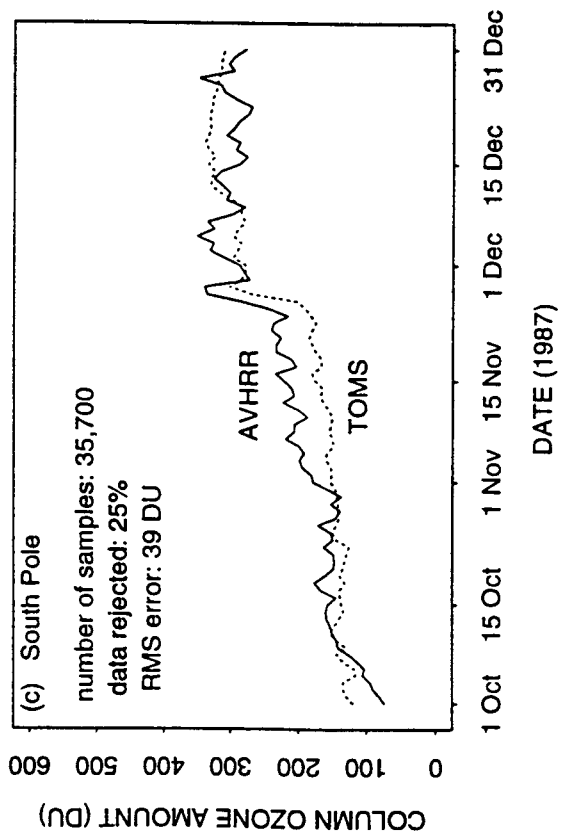
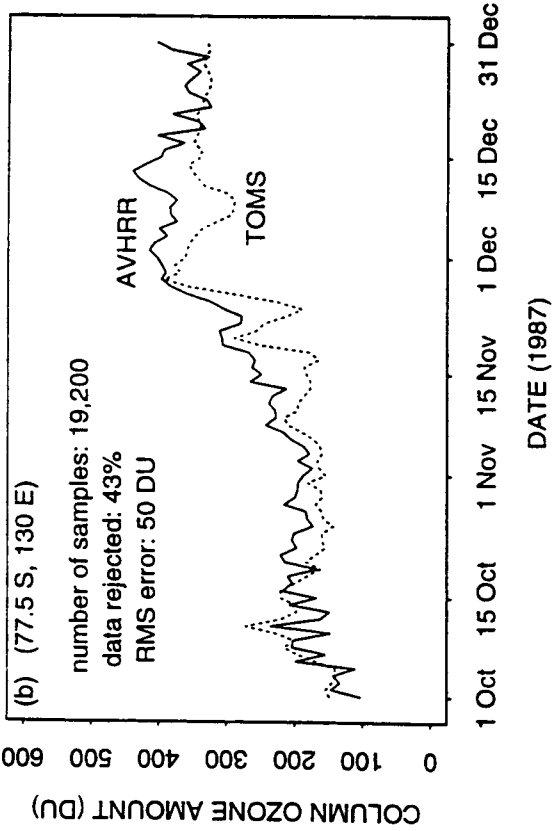
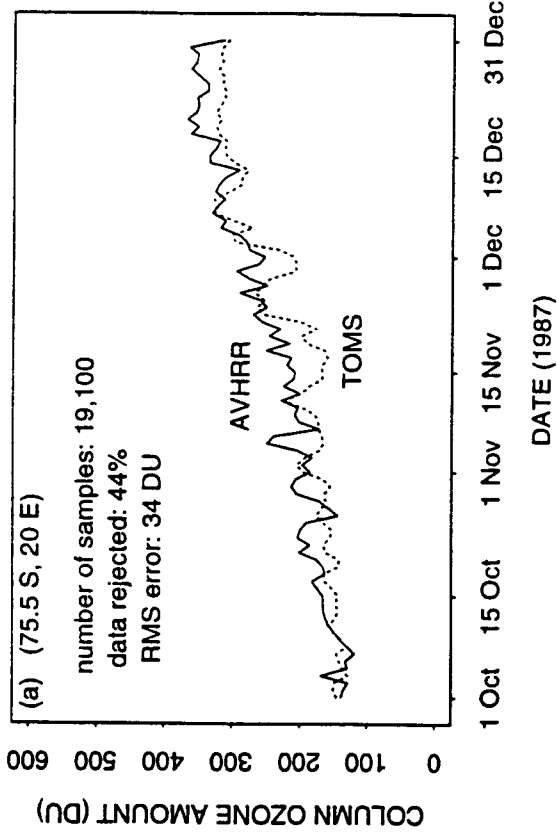


Figure 4. SECOND ALGORITHM. Time series of total ozone as in Figure 3, but omitting AVHRR data indicating extremely high or low values of reflectance (interpreted to be cloud edges).

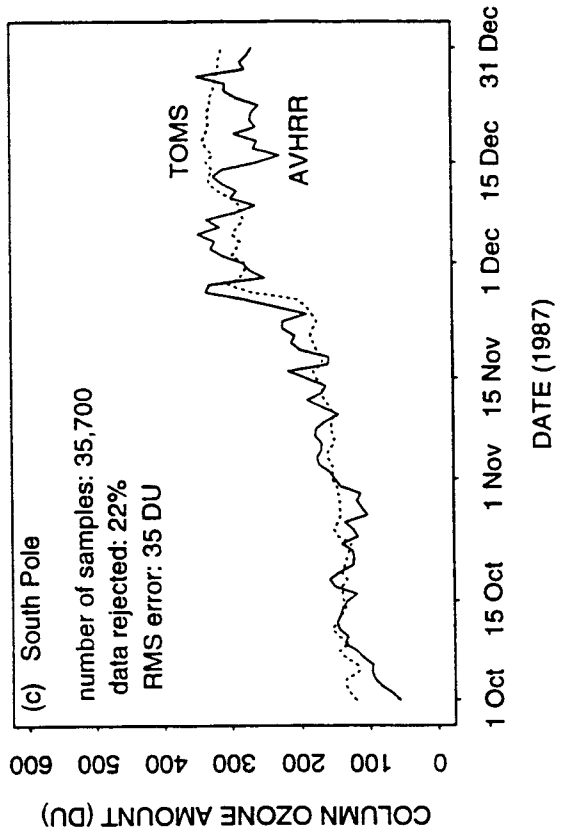
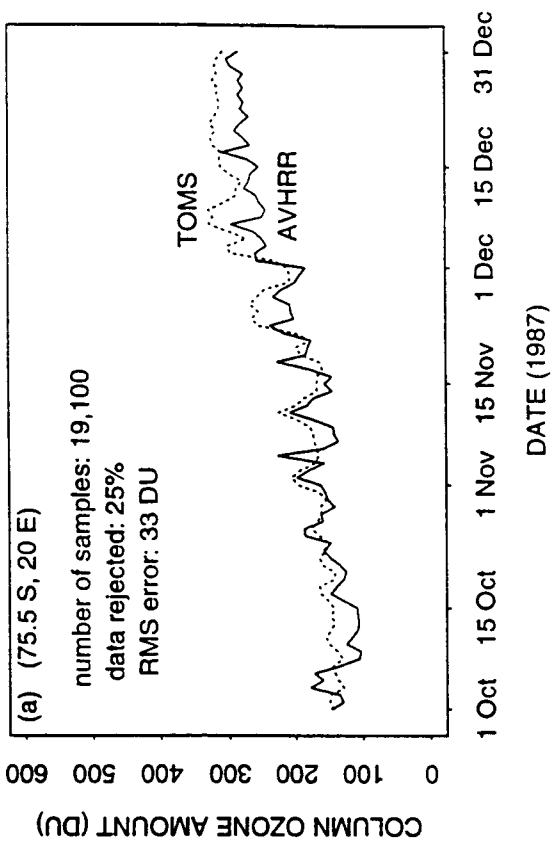
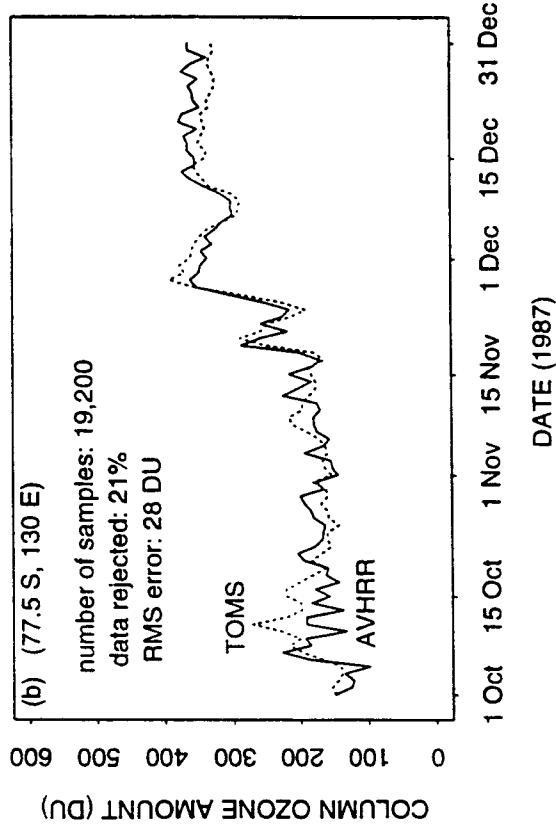


Figure 5. THIRD ALGORITHM. Time series of total ozone as in Figure 4, but using an empirical anisotropic reflectance factor $\chi(\theta_o, \theta, \phi)$ in the analysis of the AVHRR radiances.

To reduce the trend-error we need to incorporate a realistic χ into the analysis. We measured the bidirectional reflectance of surface snow from a tower at South Pole Station as the solar elevation declined in February-March 1992, and again as the sun rose during October-December 1992, for all orientations of the solar azimuth relative to the sastrugi axis. We have not yet analyzed these data to produce a χ -function which we can use for all combinations of (θ_0, θ, ϕ) . However, ignoring the effect of sastrugi orientation for the time being, we can use satellite data to develop an average empirical $\chi(\theta_0, \theta, \phi)$, as that which produces the best agreement between AVHRR-derived and TOMS-derived ozone distributions in a different year (October-December 1983).

We applied this χ function to the 1987 data; the results are plotted in Figure 5. The rms error is reduced to 28-35 DU. Also, the number of observations that were rejected by the extreme-brightness criterion is smaller in Figure 5 than in Figure 4, because of the use of an appropriate χ for each angle combination (θ_0, θ, ϕ) instead of a constant χ . The AVHRR time-series in Figure 5 are still noisier than the TOMS time-series. This suggests that averaging over a coarser spatial and/or temporal scale would be more appropriate than what we have used (100 km, 1 day).

5. CONCLUSION

By modeling the transfer of visible radiation through the Antarctic atmosphere, we have attempted to obtain column ozone from the visible channel of the AVHRR. Results of the initial investigation show promise in this technique. In future work the noise can be reduced by optimizing the spatial and temporal averaging-scales. Our direct measurements of bidirectional reflectance at the surface, together with the computed effects of Rayleigh scattering, can be used to develop a χ function for the top of the atmosphere, independent of satellite data. The small amount of absorption in Channel 1 due to water vapor and oxygen can also be taken into account, but we expect its effect be minor. To improve the method on the Antarctic Slope it will probably be necessary to consider the influence of sastrugi. If the method appears useful after these improvements have been made, the technique can be applied to Scanning Radiometer data from the 1970s.

6. ACKNOWLEDGEMENTS

2
The data in Figure 4 were provided by Dr. Arnold Gruber. This research is supported by NASA grant 1212-MDIS/BGA-014.

7. REFERENCES

1. R.D. Boime, S.G. Warren and A. Gruber, "The use of visible-channel data from NOAA satellites to measure total ozone amount over Antarctica," *Proceedings of the Quadrennial Ozone Symposium*, in press, 1993.
2. Y.L. Yung, M. Allen, D. Crisp, R.W. Zurek, and S.P. Sander, "Spatial variation of ozone depletion rates in the springtime Antarctic polar vortex," *Science*, 248, 721-724, 1990.
3. W.B. Rossow, E. Kinsella, A. Wolf, and L. Gardner, *International Satellite Cloud Climatology Project (ISCCP), Description of Reduced Resolution Radiance Data. WMO/TD No. 58*, World Meteorological Organization, Geneva, 1985.

4. G.V. Rozenberg, *Twilight; A Study In Atmospheric Optics*, 358 pp, Plenum Press, New York, 1966.
5. S.G. Warren, T.C. Grenfell, and P.C. Mullen, "Optical properties of antarctic snow," *Antarctic J. U. S.*, 21, 247-248, 1986.
6. S. Kinne and O. B. Toon, "Radiative effects of polar stratospheric clouds," *Geophys. Res. Lett.*, 17, 373-376, 1990.
7. T.R. Parish and D.H. Bromwich, "The surface windfield over the Antarctic ice sheets," *Nature*, 328, 51-54, 1987.
8. E. Vigroux, "Contribution à l'étude expérimentale de l'absorption de l'ozone," *Annales de Physique*, 8, 709-762, 1953.
9. W.J. Wiscombe and S. G. Warren, "Solar and infrared radiation calculations for the Antarctic Plateau using a spectrally-detailed snow reflectance model," *International Radiation Symposium Volume of Extended Abstracts*, 380-382, Colorado State University, Fort Collins, 1980.